JACC: BASIC TO TRANSLATIONAL SCIENCE VOL. 5, NO. 5, 2020

PRECLINICAL RESEARCH

Role of Blood Oxygen Saturation During Post-Natal Human Cardiomyocyte Cell Cycle Activities

Lincai Ye, MD, PhD,[a,b,c,*] Lisheng Qiu, MD,[a,*] Bei Feng, PhD,[a,b,c,*] Chuan Jiang, MS,[a,b] Yanhui Huang, MD,[d] Haibo Zhang, MD,[a] Hao Zhang, MD,[a,b] Haifa Hong, MD,[a,b] Jinfen Liu, MD[b]

VISUAL ABSTRACT

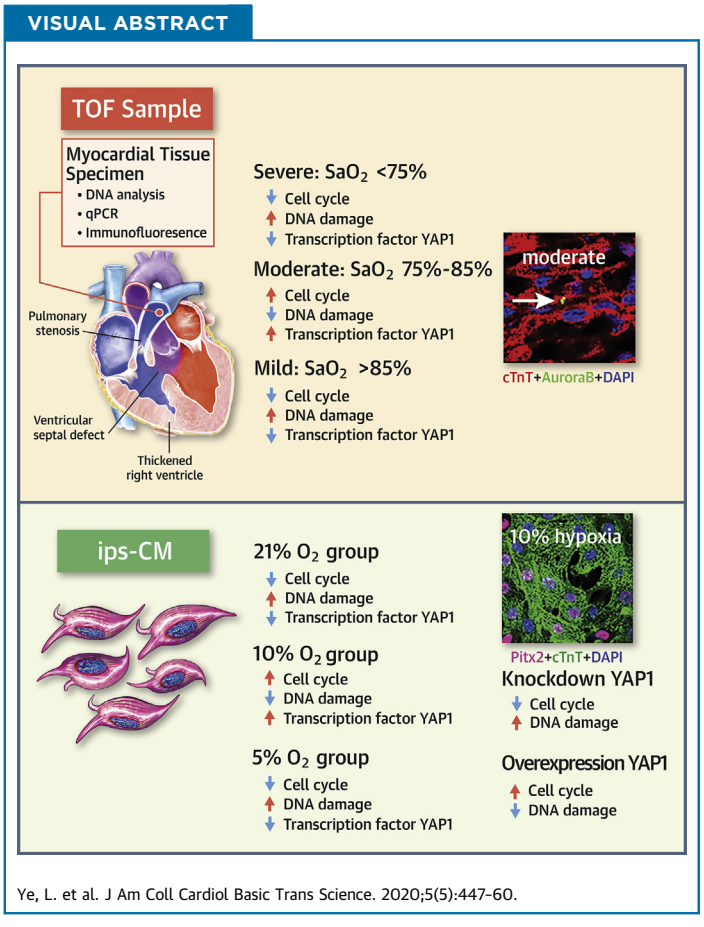

Ye, L. et al. J Am Coll Cardiol Basic Trans Science. 2020;5(5):447-60.

HIGHLIGHTS

- **This study used both human samples and iPSC-CMs to evaluate the effects of hypoxia on CM proliferation.**
- **The degree of hypoxia and the manner in which O_2 decreases both contribute to the cell cycle activity of post-natal human CMs.**
- **From the perspective of CM proliferation and protection, it has been unclear why moderate hypoxia (SaO_2:75% to 85%) is targeted by many children's medical centers when children with CHD are being transported.**
- **A target was provided that can be used for antioxidant DNA damage to protect the proliferation of post-natal human CMs.**

ISSN 2452-302X https://doi.org/10.1016/j.jacbts.2020.02.008

ABBREVIATIONS AND ACRONYMS

CHD = congenital heart disease

CM = cardiomyocytes

IF = immunofluorescence

iPSC = induced pluripotent stem cell

LV = lentivirus

O_2 = oxygen

pATM = phosphorylated ataxia telangiectasia mutated

pHH3 = phospho-histone H3

qPCR = quantitative polymerase chain reaction

SaO_2 = blood oxygen saturation

sh = short hairpin

TOF = tetralogy of Fallot

YAP1 = yes-associated protein 1

SUMMARY

Blood oxygen saturation (SaO_2) is one of the most important environmental factors in clinical heart protection. This study used human heart samples and human induced pluripotent stem cell–cardiomyocytes (iPSC-CMs) to assess how SaO_2 affects human CM cell cycle activities. The results showed that there were significantly more cell cycle markers in the moderate hypoxia group (SaO_2: 75% to 85%) than in the other 2 groups (SaO_2 <75% or >85%). In iPSC-CMs 15% and 10% oxygen (O_2) treatment increased cell cycle markers, whereas 5% and rapid change of O_2 decreased the markers. Moderate hypoxia is beneficial to the cell cycle activities of post-natal human CMs. (J Am Coll Cardiol Basic Trans Science 2020;5:447–60)

Congenital heart disease (CHD) is the leading cause of birth defect–related mortality (1,2). Although corrective surgery enables young patients to survive most forms of CHD, such patients remain at risk of developing chronic heart failure (3), which is characterized by loss of cardiomyocytes (CMs). In addition, after cardiopulmonary bypass, it is possible that these patients will experience low cardiac output syndrome due to anoxia-induced CM impairment. Low cardiac output syndrome is one of the most serious physiological abnormalities arising from cardiac surgery (4). Recently, our research group (along with other groups) showed that there were significantly more cell cycle active CMs in young patients (5–7). Furthermore, CMs are important contributors to post-natal heart growth (7). Thus, it is essential that young CMs are protected and that their limited proliferative function is maintained during CHD surgery.

Blood oxygen saturation (SaO_2) is one of the most important indexes of heart and brain protection during the peri-operative period (8). However, oxygen (O_2) is deemed a "double-edged sword" when it comes to cardiac function and repair (9); the effects of hypoxia on CM proliferation are associated with its stage of development (10). Paradis et al. (11) reported that hypoxia/anoxia in newborns inhibits CM proliferation. Conversely, Puente et al. (12) showed that the O_2-rich post-natal environment induces CM cell cycle arrest, whereas hypoxia facilitates the proliferation of young CMs. One possible explanation for the conflicting results between these 2 studies is that they used different methods. Paradis et al. (11) exposed neonatal mice to an environment that contained approximately 0.2% O_2 for d10 min, whereas Puente et al. (12) exposed mice to an environment that contained approximately 15% O_2 for 7 days. It is likely that too much or too little O_2 inhibits the cell cycle activities of CMs, and that a moderate supply of O_2 represents a more optimal scenario. This is also why many children's centers aim to supply moderate levels of SaO_2 during transportation (13).

When O_2 levels increase, mitochondrial oxidative phosphorylation increases accordingly. This phenomenon facilitates increased free radical production, causing increased DNA damage (14,15). Conversely, severe hypoxia results in the down-regulation of antioxidant defenses, making cells vulnerable to oxidative damage and promoting

From the [a]Department of Thoracic and Cardiovascular Surgery, Shanghai Children's Medical Center, Shanghai Jiaotong University School of Medicine, Shanghai, China; [b]Shanghai Institute for Pediatric Congenital Heart Diseases, Shanghai Children's Medical Center, Shanghai Jiaotong University School of Medicine, Shanghai, China; [c]Institute of Pediatric Translational Medicine, Shanghai Children's Medical Center, Shanghai Jiaotong University School of Medicine, Shanghai, China; and the [d]Department of Anesthesiology, Shanghai Children's Medical Center, Shanghai Jiaotong University School of Medicine, Shanghai, China. *Drs. Ye, Qiu, and Feng contributed equally to this work and are co-first authors. This work was supported by the National Natural Science Foundation of China (81670287, 81800285, and 81570281), the National Key R&D Program of China (2019YFA0110401), Foundation of Pudong Science and Technology Development (PKJ2016-Y35 and PKJ2019-Y12), Foundation of Shanghai Health and Family Planning Committee (20164Y0106), and the National Basic Research Program of China (2013CB945304), and the Key Discipline Group Development Fund of Health and Family Planning Commission of Pudong New District (PWZxq2017-14). The authors have reported that they have no relationships relevant to the contents of this paper to disclose.

The authors attest they are in compliance with human studies committees and animal welfare regulations of the authors' institutions and Food and Drug Administration guidelines, including patient consent where appropriate. For more information, visit the *JACC: Basic to Translational Science* author instructions page.

Manuscript received September 27, 2019; revised manuscript received February 12, 2020, accepted February 13, 2020.

increased DNA damage (16,17). Current evidence suggests that DNA damage is a critical factor in the suppression of CM proliferation (12,18). We speculated that dramatic increases or decreases in postnatal O_2 contribute to an increase in mitochondrial content, thereby activating the DNA damage response and causing permanent cell cycle arrest in CMs.

Yes-associated protein 1 (YAP1) is closely related to the regulation of CM proliferation (19–21). For example, the study by van Gise et al (20) demonstrated that activated YAP1 can promote the proliferation of mouse CMs after birth, and our previous studies showed that YAP1 plays an important role in the post-natal proliferation of human CMs (6). Studies on neuronal cells have shown that YAP1 degradation plays an important role in DNA oxidative damage by inhibiting neuronal cell proliferation (22,23). For example, Lehtinen et al. (22) and Xiao et al. (23) demonstrated that O_2 free radical-mediated DNA damage could activate the Hippo/mammalian STE20-like protein kinase (MST) signaling pathway, which, in turn, phosphorylates and leads to the degradation of YAP1, and ultimately, to the inhibition of neuronal cell proliferation (22,23). Thus, we also set out to investigate the role of YAP1 in hypoxia-induced CM proliferation.

METHODS

Primers, reagents, and antibodies are detailed in Supplemental Tables S1 and S2.

STUDY POPULATION AND TISSUE SAMPLING. We collected 30 right ventricular outflow myocardial tissue specimens from resections that were required to relieve obstruction in patients with tetralogy of Fallot (TOF) at the Shanghai Children's Medical Center (Shanghai, China) between January 2018 and July 2018. Each specimen was preserved in liquid nitrogen and later divided into 3 portions, which were used for DNA extraction, quantitative polymerase chain reaction (qPCR), and immunofluorescence (IF). All procedures conformed to the principles outlined in the Declaration of Helsinki and were approved by The Animal Welfare and Human Studies Committee at the Shanghai Children's Medical Center. Parental written informed consent was obtained before study initiation.

CM DIFFERENTIATION, MAINTENANCE, AND O_2 TREATMENT OF HUMAN-INDUCED PLURIPOTENT STEM CELLS. We purchased the human-induced pluripotent stem cell (iPSC) line del-AR1034ZIMA 001 from Allele Biotechnology (San Diego, California). The cells were differentiated under normal O_2 conditions and maintained with the STEMdiff Cardiomyocyte Differentiation Kit (STEMCELL Technologies, Vancouver, British Columbia, Canada) according to the manufacturer's instructions. After 15-day induction, approximately 90% of the cells were beating and positive for both cardiac troponin T and sarcomeric α-actinin. We re-seeded the cells and cultured them in different O_2 concentrations (21%, 15%, 10%, and 5%) in incubators for 7 days. To produce rapid changes in O_2, we incubated cells at 21% O_2 for 2 days, and then changed the O_2 level to 15% for 2 days, 10% for 2 days, and finally, 5% for 2 days. After 7 days of culture, we subjected the cells to DNA extraction, qPCR, and IF.

YAP1 OVEREXPRESSION BY ADENOVIRUS HARBORING YAP1—COMPLEMENTARY DNA. We purchased YAP1 complementary DNA and negative control lentiviral vector from GeneChem (Shanghai, China). YAP1-complementary DNA or negative control was cloned into pDC315 plasmid (GeneChem) harboring the cytomegalovirus promoter. The pDC315-YAP1 plasmid or control plasmid was co-transfected with pBHGloxΔE1,3Cre (GeneChem) into HEK293 cells using Lipofectamine 2000 (Invitrogen, Waltham, Massachusetts). After 2 rounds of virus amplification, the supernatant was filtered at 0.45 μm, and purified using the Adeno-XTM Virus Purification kit (Takara, Clontech, Dalian, China). YAP1 adenovirus transfections were performed over 8 h and confirmed by Western blotting and IF. At 72 h after transfection, we cultured the cells in incubators at an O_2 concentration of 5% for 7 days. After washing cells with phosphate-buffered saline, they were harvested and subjected to qPCR, Western blotting, and IF.

YAP1 KNOCKDOWN BY LENTIVIRUS HARBORING YAP SHORT-HAIRPIN RNA. Short-hairpin (sh) RNA (shYAP1:5′-GACTCAGGATGGAGAAATTTA-3′) targeting a specific region of human YAP1 mRNA (NM_006106), and a scrambled negative control (sh-con, 5′-TTC TCC GAA CGT GTCACG T-3′), were cloned into the GV248 vector (GeneChem). Lentivirus (LV) gene transfer vectors encoding gene fluorescent protein (GFP)-shYAP1 (LV-GFP-shYAP1) and a scrambled shRNA used as the negative control (LV-GFP-sh-con) were synthesized by GeneChem. Transfections were performed over 8 h and confirmed by Western blotting and IF. At 72 h after transfection, cells were cultured in incubators at an O_2 concentration of 10% for 7 days. After washing cells with phosphate-buffered saline, we harvested the cells and subjected to them qPCR, Western blotting, and IF.

IF. Slides or cells were washed 3 times with phosphate-buffered saline, fixed with 4%

paraformaldehyde for 10 min, permeated with 0.5% Triton X-100 for 15 min, blocked in 10% donkey serum for 30 min, and stained with primary antibodies overnight at 4° C. After an additional 3 washes, we incubated the sections or cells with secondary antibodies and 4′,6-diamidino-2-phenylindole for 30 min. Three researchers who were blinded to the sample identity quantified cellular Ki67, phospho-histone H3 (pHH3), and aurora B by either manual counting or digital thresholding (image segmentation and creation of a binary image from a grayscale). We analyzed the converted binary images using ImageJ software (National Institutes of Health, Bethesda, Maryland).

qPCR ANALYSIS. For mRNA quantification, mRNA was extracted and purified using the PureLink RNA Micro Scale Kit (Life Technologies, Carlsbad, California). Reverse transcription was performed using the PrimeScriptTM reagent kit. The qPCR reactions were carried out using SYBR Green Power Premix Kits (Applied Biosystems, Foster City, California) according to the manufacturer's instructions. The reactions were performed with the 7900 Fast Real-Time PCR System (Applied Biosystems) under the following conditions: 1 cycle at 95°C for 10 s, followed by 40 cycles of 95°C for 15 s, and 60°C for 60 s. The primers were obtained from Generay Biotech Co., Ltd (Shanghai, China).

For mitochondrial DNA quantification (24), DNA was extracted and purified from tissue samples following proteinase K digestion and phenol and/or chloroform extraction. Mitochondrial DNA was quantified by qPCR, and quantification was performed using the SYBR Green PCR Master Mix and 7900 Sequence Detection System (Applied Biosystems). The relative mitochondrial DNA copy number was calculated from the ratio of mitochondrial DNA copies to nuclear DNA copies per gram of tissue. Then the relative fold change was then calculated using the ΔΔCT method.

WESTERN BLOT ANALYSIS. Proteins were extracted with Radio Immunoprecipitation Assay (RIPA) (Beyotime, Shanghai, China) Lysis Buffer according to the manufacturer's instruction, separated on 10% sodium dodecyl sulfate(SDS) (Beyotime, Shanghai, China) polyacrylamide gels, and transferred onto polyvinylidene fluoride membranes (Merck, Millipore, Billerica, Massachusetts). Then, the membranes were blocked in 5% nonfat milk in Tris-buffered saline with Tween 20 for 1 h at room temperature and incubated with primary antibodies overnight at 4°C. After 3 washes with Tween 20, the membranes were incubated with second antibodies for 1 h at room temperature, and proteins were detected using the Bio-Rad ChemiDoc Imaging Systems (Bio-Rad, Hercules, California).

STATISTICAL METHODS. Continuous data were expressed as mean ± SD. Differences were tested with 1-way analysis of variance test and Student's Newman-Keuls for post hoc test. Categorical variables were compared by the Wilcoxon test. The values of $p < 0.05$ were considered statistically significant. Statistical analyses were performed using SAS (software version 9.4, SAS Institute Inc., Cary, North Carolina).

RESULTS

BASELINE PATIENT CHARACTERISTICS. Thirty infants with TOF were included in the study. Because age and pressure load could affect CM proliferation (6,8,15), patients were selected to ensure that there were no significant differences in age, sex, or pulmonary arterial pressure (increasing right ventricular pressure load) among the 3 groups (Supplemental Table S3). The only factor that significantly differed among the groups was SaO_2 ($p < 0.001$; $n = 10$). In clinical practice, patients were divided into 3 groups according to SaO_2 levels: >85% was defined as mild hypoxia (group A); 75% to 85% was defined as moderate hypoxia (group B); and <75% was defined as severe hypoxia (group C) (13). Ten patients from each group were analyzed to test our hypothesis that SaO_2 influenced CM cell cycle activities. Patient characteristics were deemed well balanced and suitable for studying the effects of SaO_2 on CM cell cycle activities.

CELL CYCLE ACTIVITY OF CMs IN THE DIFFERENT SaO_2 GROUPS. Because Ki67 is present during all active phases of the cell cycle (G1, S, G2, and mitosis), we measured Ki67-positive cells in all 3 groups. As shown in **Figures 1A and 1B**, the percentage of Ki67-positive CMs in groups A, B, and C was 0.99 ± 0.25%, 6.08 ± 2.51%, and 2.47 ± 2.64%, respectively ($p < 0.001$), which suggested that cell cycle activities in those with moderate hypoxia CMs were upregulated. Next, we detected the mitotic marker pHH3 and found that the percentages of pHH3-positive CMs in groups A, B, and C was 0.10 ± 0.04%, 0.53 ± 0.13%, and 0.23 ± 0.10%, respectively ($p < 0.001$) (**Figures 1C and 1D**). This indicated that CMs in the mitotic stage in group B also increased, although the percentage of pHH3-positive CMs was only 10% of Ki67-postive CMs. A combination of aurora B–positive, midbody position, and daughter nuclei distance that indicated CM proliferation was recently demonstrated (25), so we also counted aurora B–positive CMs. None was found in most of the sections from groups A and C (mild and severe hypoxia, respectively), but the

FIGURE 1 Higher Cell Cycle Activity of Human CMs in Moderate SaO_2 Conditions

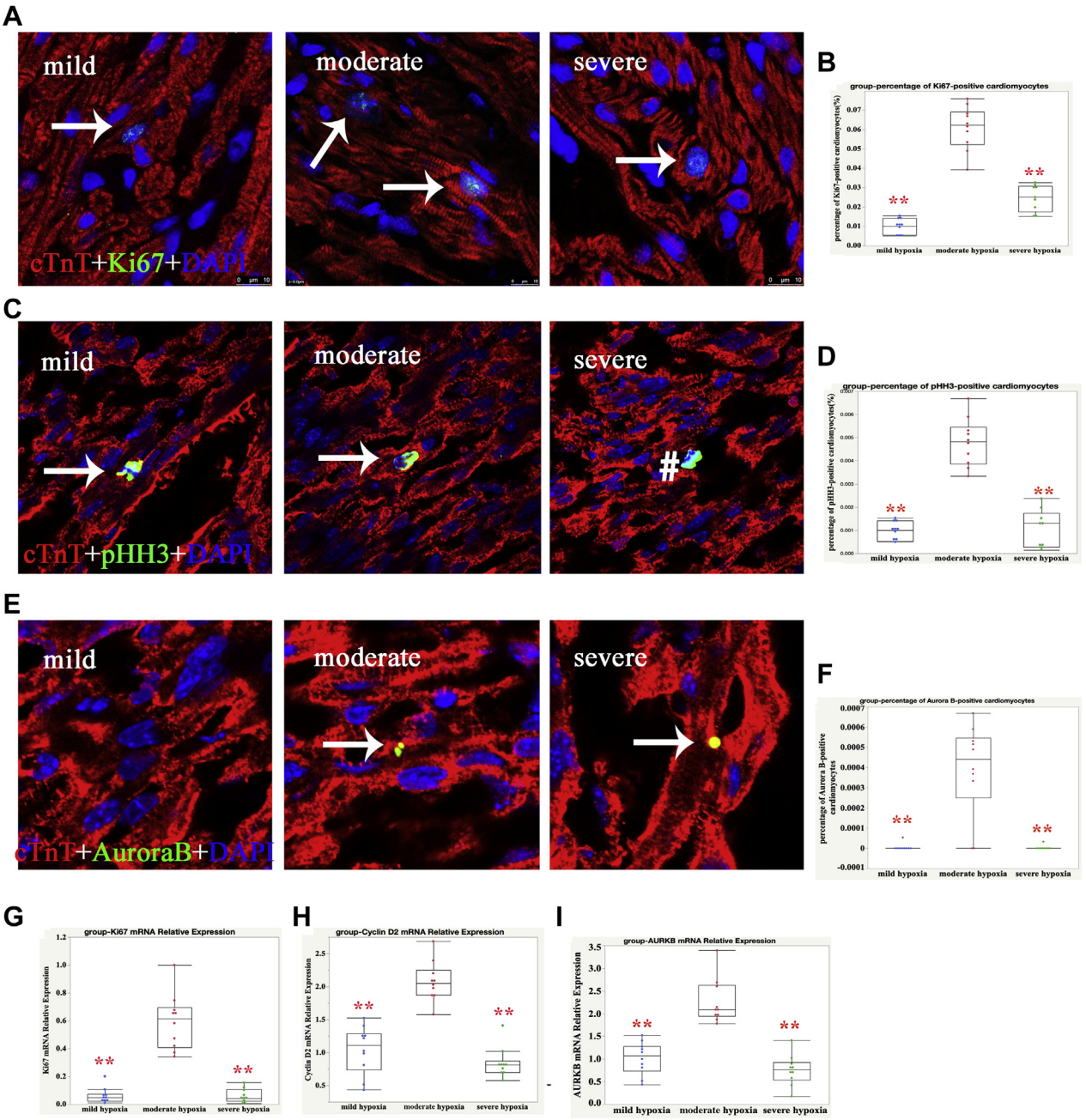

(A) Representative Ki67-positive cardiomyocytes (CMs) in group B; cardiac troponin-T (cTnT) **(red)**, Ki67 **(green)**, and 4′,6-diamidino-2-phenylindole (DAPI) **(blue)** stainings are shown. The **arrow** indicates proliferating CMs. **(B)** Quantification of Ki67-positive CMs: 1-way analysis of variance (ANOVA), Student Newman Keuls (SNK), n = 10; **p < 0.01. **(C)** Representative phospho-histone H3 (pHH3)−positive CMs in group B; cTnT **(red)**, pHH3 **(green)**, and DAPI **(blue)** stainings are shown; the **arrow** indicates proliferating CMs and **hatch sign** indicates proliferating non-CMs. **(D)** Quantification of pHH3-positive CMs; 1-way ANOVA, SNK, n = 10; **p < 0.01. **(E)** Representative aurora B-positive CMs in group B; cTnT **(red)**, aurora B **(green)**, and DAPI **(blue)** stainings are shown; the **arrow** indicates proliferating CMs. **(F)** Quantification of aurora B-positive CMs; 2-way ANOVA, SNK, n = 10; **p < 0.01. We used quantitative polymerase chain reaction (qPCR) to analyze the expression of mRNA levels of **(G)** Ki67, **(H)** cyclin D2, and **(I)** AURKB in CMs treated with different levels of oxygen saturation (SaO_2). Our results indicated that *Ki67*, *cyclin D2*, and *AURKB* mRNA were significantly increased in the moderate SaO_2 group compared with the other 2 groups. Glyceraldehyde-3-phosphate dehydrogenase (GAPDH) served as a control; 1-way ANOVA, SNK, n = 10; **p < 0.01.

percentage of aurora B–positive CMs in group B was 0.04 ± 0.03% (Figures 1E and 1F). These results indicated that moderate SaO_2 levels promoted CM proliferation.

To confirm these results, we also performed qPCR to detect the mRNA levels of *Ki67*, *cyclin D2*, and *aurora B*. As shown in Figures 1G to 1I, the relative expression of *Ki67*, *cyclin D2*, and *aurora B* (*AURKB*) in group B was significantly increased. This result confirmed that moderate SaO_2 increased the cell cycle activities of CMs.

CELL CYCLE ACTIVITY OF HUMAN iPSC-CMs CULTURED AT DIFFERENT O_2 CONCENTRATIONS

The previously mentioned results suggested that moderate SaO_2 was beneficial to CM cell cycle activity; however, it remains unclear if this is true in vitro. Therefore, we set up 5 different O_2 concentrations and treatment methods to observe the effect of SaO_2 on CM proliferation. As shown in Figure 2, 15% O_2 and 10% O_2 treatment for 7 days significantly increased the percentage of Ki67-, pHH3-, and aurora B–positive CMs, whereas 5% O_2 and rapidly changing O_2 (21% to 5%) treatment decreased this percentage compared with normal O_2 (21%) treatment. This suggested that both O_2 concentrations and treatment methods contributed to the cell cycle activities of human iPSC-CMs in vitro. The percentage of Ki67-positive human iPSC-CMs cultured in vitro in normal O_2 was as high as 20%, which suggested that the cell cycle activity of iPSC-CMs in vitro was much higher than that of human CMs in vivo.

REDUCED OXIDATIVE DNA DAMAGE IN MODERATE SaO_2-TREATED CMs. Puente et al. (12) previously reported that reduced mitochondrial DNA content might be an indicator of reduced oxidative DNA damage. The latter form of damage is a critical inhibitor of cell proliferation. In this study, we analyzed mitochondrial DNA content in heart tissue from patients with TOF. As expected, mitochondrial DNA levels were significantly reduced in the moderate SaO_2 group compared with the other 2 groups (Figure 3A), which suggested that moderate SaO_2 levels might protect CMs by inhibiting DNA damage. To validate this result, we monitored levels of 8-oxoguanine (one of the most common DNA lesions that results from reactive oxygen species) in all 3 groups (26). As shown in Figures 3B and 3C, 8-oxoguanine levels were significantly reduced in the moderate SaO_2 group. We also detected a DNA damage response marker, namely, phosphorylated ataxia telangiectasia mutated (pATM). Similarly, pATM levels were significantly reduced in the moderate SaO_2 group (Figures 3D and 3E). Because paired like homeodomain 2 (Pitx2) is a critical antioxidant factor and promotes CMs proliferation (27), we also detected its expression in the 3 different SaO_2 groups. The results showed that Pitx2 was significantly upregulated in the moderate SaO_2 group (Figures 3F and 3I). These results suggested that moderate SaO_2 levels facilitated the protection of CMs by reducing DNA damage.

In accordance with the cell cycle activity of human iPSC-CMs cultured at different levels of O_2, expression of 8-oxoguanine, mitochondrial DNA, and pATM was reduced in the 15% and 10% O_2-treated groups but was increased in the 5% and 21% to 5% O_2-treated groups compared with the normal O_2-treated groups (Figures 4A to 4E). The expression of Pitx2 was upregulated in the 15% and 10% O_2-treated groups but was downregulated in the 5% and 21% to 5% O_2-treated groups compared with the normal O_2-treated groups (Figures 4F to 4I).

HIGHER EXPRESSION AND OVEREXPRESSION OF YAP1. Higher expression of YAP1 occurred in the moderate hypoxia group, overexpression of YAP1 rescued the cell cycle activities of human iPSC-CMs in the 5% O_2-treated group, and knockdown reduced activities in the 10% O_2-treated group

YAP1 is a critical co-transcription factor in the regulation of CM proliferation. To investigate its role in inhibiting oxidative DNA damage to CMs, we first investigated the expression of YAP1 in human heart samples. We found a significant increase of YAP1 expression in the moderate SaO_2 group compared with the other 2 groups (Figures 5A and 5B). Consistent with our observations in heart samples, there was also more abundant expression of YAP1 in the 10% O_2-cultured human iPSC-CMs, especially in the nuclei (Figures 5C and 5E). When YAP1 was overexpressed in 5% O_2-treated iPSC-CMs (Figures 5F to 5H), the percentage of Ki67-, pHH3-, and aurora B–positive CMs significantly increased (Figures 5I and 5J) ($p < 0.01$; $n = 10$). In contrast, when YAP1 was knocked down in 10% O_2-treated iPSC-CMs (Figures 5K to 5M), the percentage of Ki67-, pHH3-, and aurora B–positive CMs was significantly reduced (Figures 5O and 5P) ($p < 0.01$; $n = 10$).

REDUCED OXIDATIVE DNA DAMAGE AFTER OVEREXPRESSION OF YAP1 IN HUMAN iPSC-CMs CULTURED IN 5% O_2. To cross-check the effects of YAP1 overexpression, we detected mitochondrial DNA and 8-oxoguanine expression in human iPSC-CMs and found that both markers were downregulated in the YAP1 overexpression group (Figures 6A to 6C).

FIGURE 2 Higher Cell Cycle Activity of Human iPSC-CMs in 10% and 15% O_2-Treated Conditions

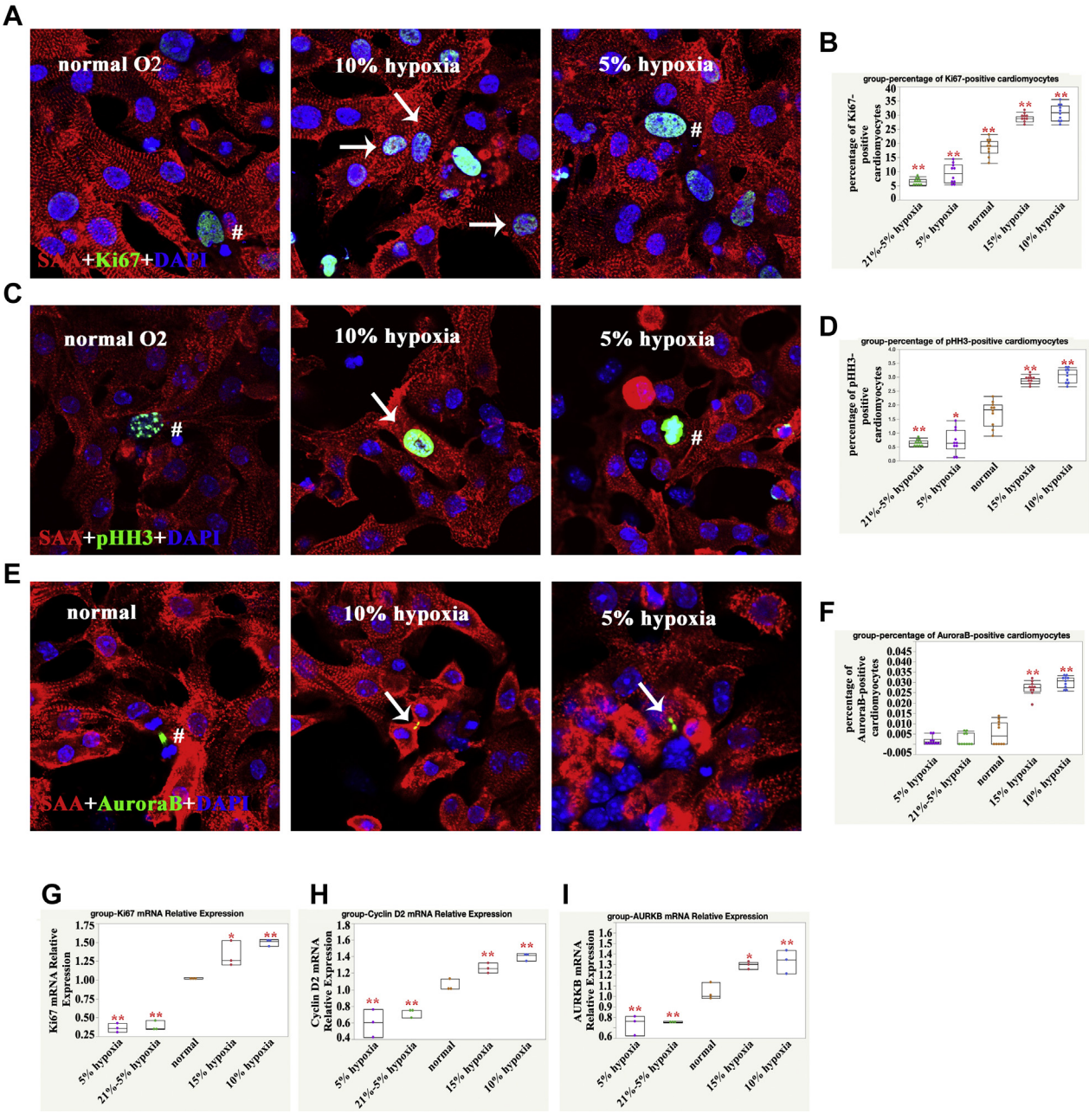

(A) Ki67-positive CMs, sarcomeric α-actinin (SAA) **(red)**, Ki67 **(green)**, and DAPI **(blue)** stainings are shown; the **arrow** indicates proliferating CMs, and the **hatch sign** indicates proliferating non-CMs. **(B)** Quantification of Ki67-positive CMs for each group: 1-way ANOVA, SNK; $^{**}p < 0.01$, n = 10 fields for each group from 3 independent experiments. **(C)** pHH3-positive CM: SAA **(red)**, pHH3 **(green)**, and DAPI **(blue)** are shown; the **arrow** indicates proliferating CMs, and the **hatch sign** indicates proliferating non-CMs. **(D)** Quantification of pHH3-positive CMs for each group: 1-way ANOVA, SNK; $^{**}p < 0.01$, n = 10 fields for each group from 3 independent experiments. **(E)** Aurora B-positive CM: SAA **(red)**, aurora B **(green)**, and DAPI **(blue)** stainings are shown; the **arrow** indicates proliferating CMs, and the **hatch sign** indicates proliferating non-CMs. **(F)** Quantification of aurora B-positive CMs for each group: 1-way ANOVA, SNK; $^{**}p < 0.01$, n = 10 fields for each group from 3 independent experiments. We used qPCR to analyze mRNA levels of **(G)** *Ki67*, **(H)** *cyclin D2*, and **(I)** *AURKB* in CMs treated with different levels of oxygen (O_2). Our results indicated that *Ki67*, *cyclin D2*, and *AURKB* mRNA were significantly increased in 15% and 10% O_2-treated human induced pluripotent stem cell–cardiomyocytes (iPSC-CMs). GAPDH served as a control; 1-way ANOVA, SNK, n = 3; $^{*}p < 0.05$; $^{**}p < 0.01$. Abbreviations as in Figure 1.

FIGURE 3 Oxidative DNA Damage Was Significantly Reduced in Moderate Hypoxia Human CMs

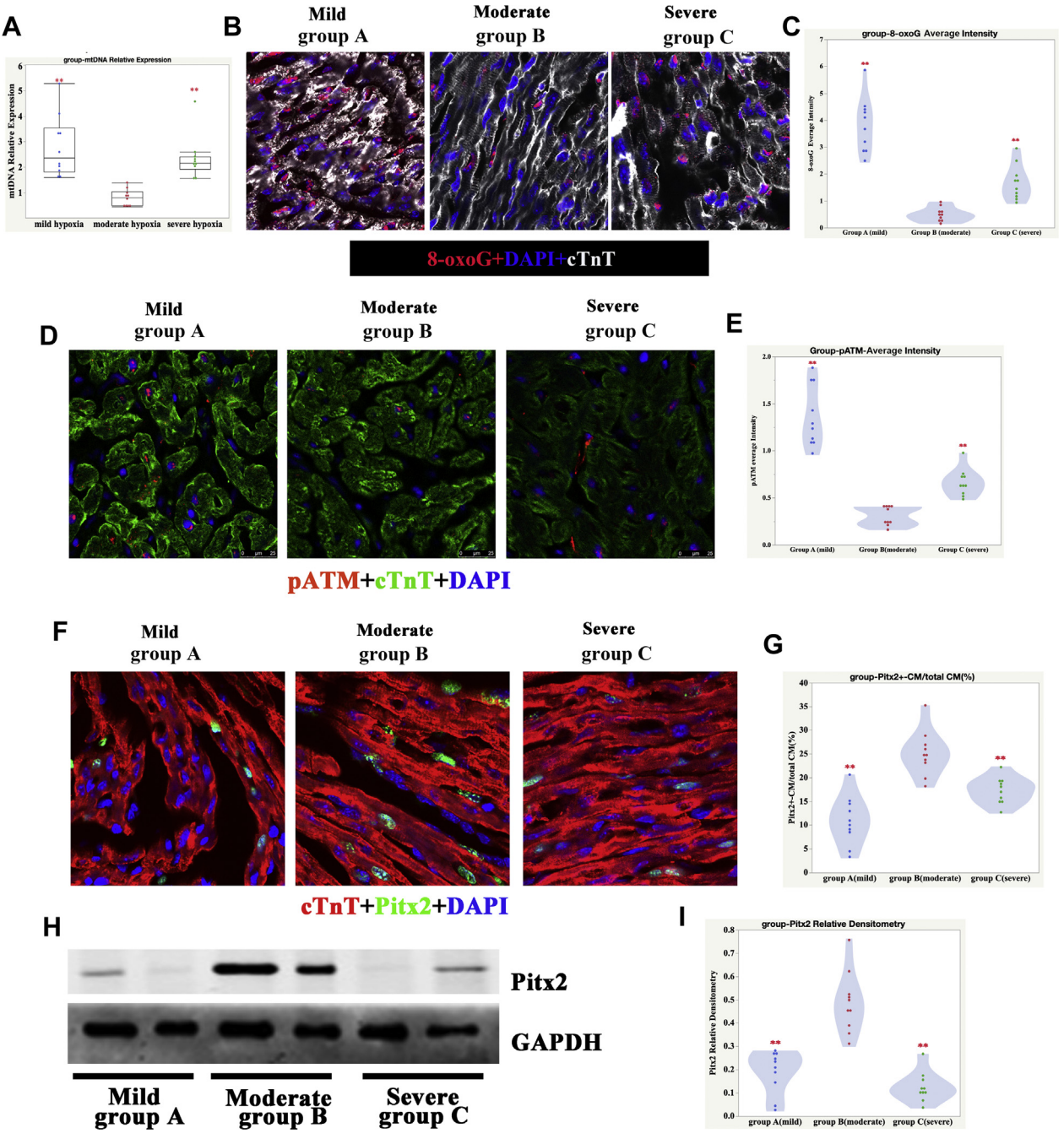

(A) We used qPCR to analyze mitochondrial DNA (mtDNA) levels in the hearts of patients with tetralogy of Fallot (TOF). Our results indicated that mtDNA was significantly decreased in the moderate SaO_2 group compared with the other 2 groups: 1-way ANOVA, SNK, n = 10 samples; **p < 0.01. (B) 8-oxoguanine (8-oxoG) in mild, moderate, and severe hypoxia heart samples; cTnT **(white)**, 8-oxoG **(red)**, and DAPI **(blue)** stainings are shown. **(C)** Quantification of 8-oxoG immunofluorescence (IF) intensity in mild, moderate, and severe hypoxia heart samples: 1-way ANOVA, SNK, n = 10 samples, **p < 0.01, compared with group B (moderate hypoxia). **(D)** Phosphorylated ataxia telangiectasia mutated (pATM) in mild, moderate, and severe hypoxia heart samples; cTnT **(green)**, pATM **(red)**, and DAPI **(blue)** staining are shown. **(E)** Quantification of pATM IF intensity in mild, moderate, and severe hypoxia heart samples. One-way ANOVA, SNK, n = 10 samples; **p < 0.01, compared with group B (moderate hypoxia). **(F)** IF graph of Pitx2 in mild, moderate, and severe hypoxia heart samples; cTnT **(red)**, Pitx2 **(green)**, and DAPI **(blue)** staining are shown. **(G)** Quantification of Pitx2-positive CMs in mild, moderate, and severe hypoxia heart samples. One-way ANOVA, SNK, n = 10 samples; **p < 0.01, compared with group B (moderate hypoxia). **(H)** Western blot graph of Pitx2 in mild, moderate, and severe hypoxia heart samples. **(I)** Quantification of Pitx2 densitometry in mild, moderate, and severe hypoxia heart samples. One-way ANOVA, SNK, n = 10 samples; **p < 0.01, compared with group B (moderate hypoxia). Abbreviations as in Figures 1 and 2.

FIGURE 4 Oxidative DNA Damage Was Significantly Reduced in 10% and 15% O_2-Treated Human iPSC-CMs

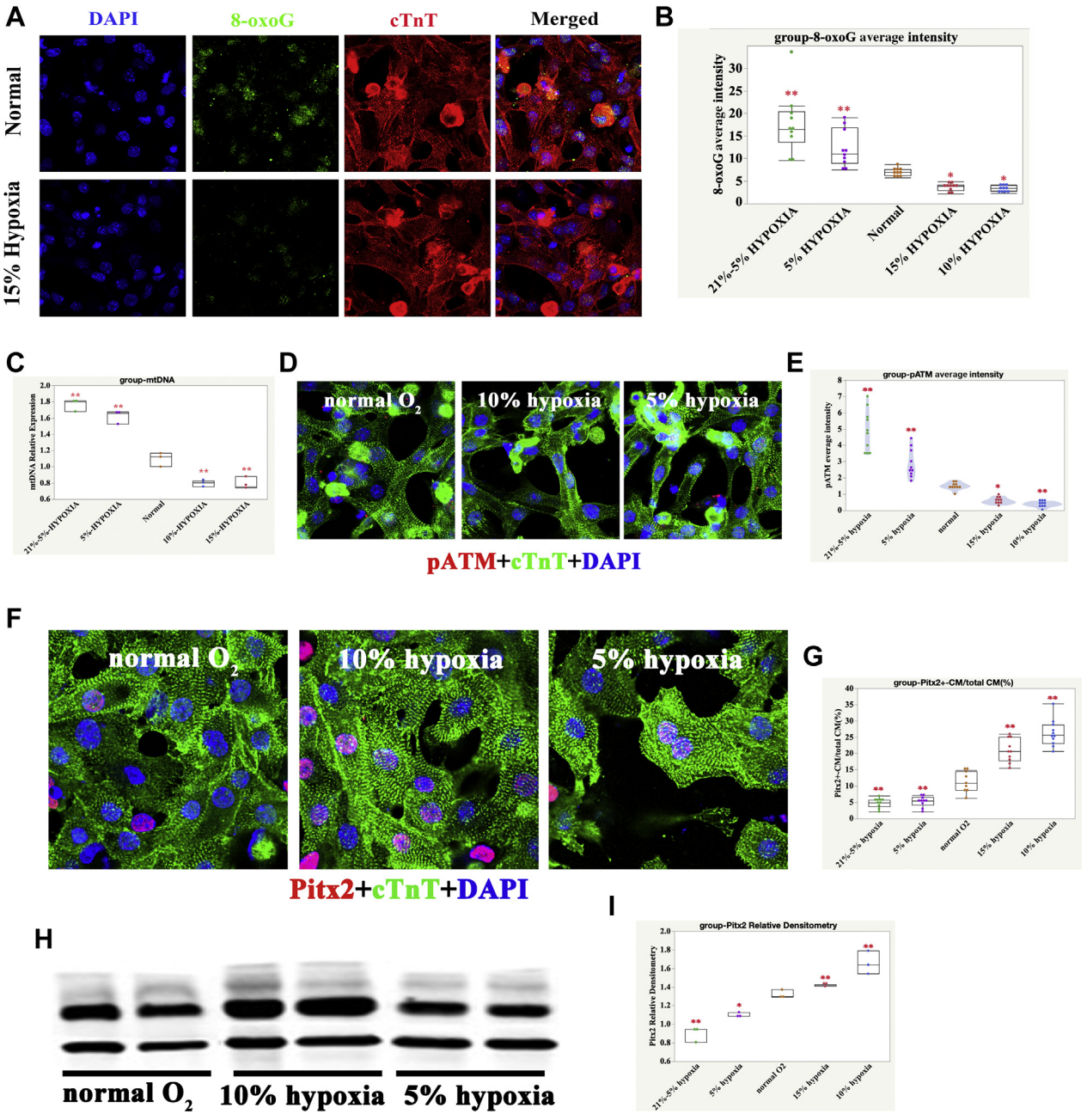

(A) 8-oxoG in normal and 15% O_2-Treated Human iPSC-CMs; cTnT **(red)**, 8-oxoG **(green)**, and DAPI **(blue)** stainings are shown. **(B)** Quantification of 8-oxoG IF intensity in differently O_2-treated human iPSC-CMs; 1-way ANOVA, SNK; *$p < 0.05$; **$p < 0.01$, n = 10 fields from 3 independent experiments, compared with normal. **(C)** Quantification of mtDNA content in differently O_2-treated human iPSC-CMs; 1-way ANOVA, SNK; **$p < 0.01$, n = 3 replicates compared with normal. **(D)** pATM in normal, 10%, and 5% O_2-treated human iPSC-CMs; cTnT **(green)**, pATM **(red)**, and DAPI **(blue)** stainings are shown. **(E)** Quantification of pATM IF intensity in differently O_2-treated human iPSC-CMs; 1-way ANOVA, SNK; *$p < 0.05$; **$p < 0.01$, n = 10 fields from 3 independent experiments compared with normal. **(F)** IF graph of Pitx2 in normal, 10% hypoxia, and 5% hypoxia iPSC-CMs; cTnT **(green)**, Pitx2 (**red**), and DAPI **(blue)** staining are shown. **(G)** Quantification of Pitx2 positive CMs in normal, 10% hypoxia, and 5% hypoxia iPSC-CMs. One-way ANOVA, SNK, n = 10 fields from 3 independent experiments; **$p < 0.01$, compared with group B (moderate hypoxia). **(H)** Western blot graph of Pitx2 in normal, 10% hypoxia, and 5% hypoxia iPSC-CMs. **(I)** Quantification of Pitx2 densitometry in normal, 10% hypoxia, and 5% hypoxia iPSC-CMs. One-way ANOVA, SNK, n = 3 samples; **$p < 0.01$, compared with group B (moderate hypoxia). Abbreviations as Figures 1 to 3.

FIGURE 5 Higher Expression of YAP1 in Moderate SaO_2 Human CMs and 10% O_2-Treated Human iPSC-CMs; Overexpression of YAP1 Protected the Proliferative Potential of Human iPSC-CMs From Oxidative DNA Damage

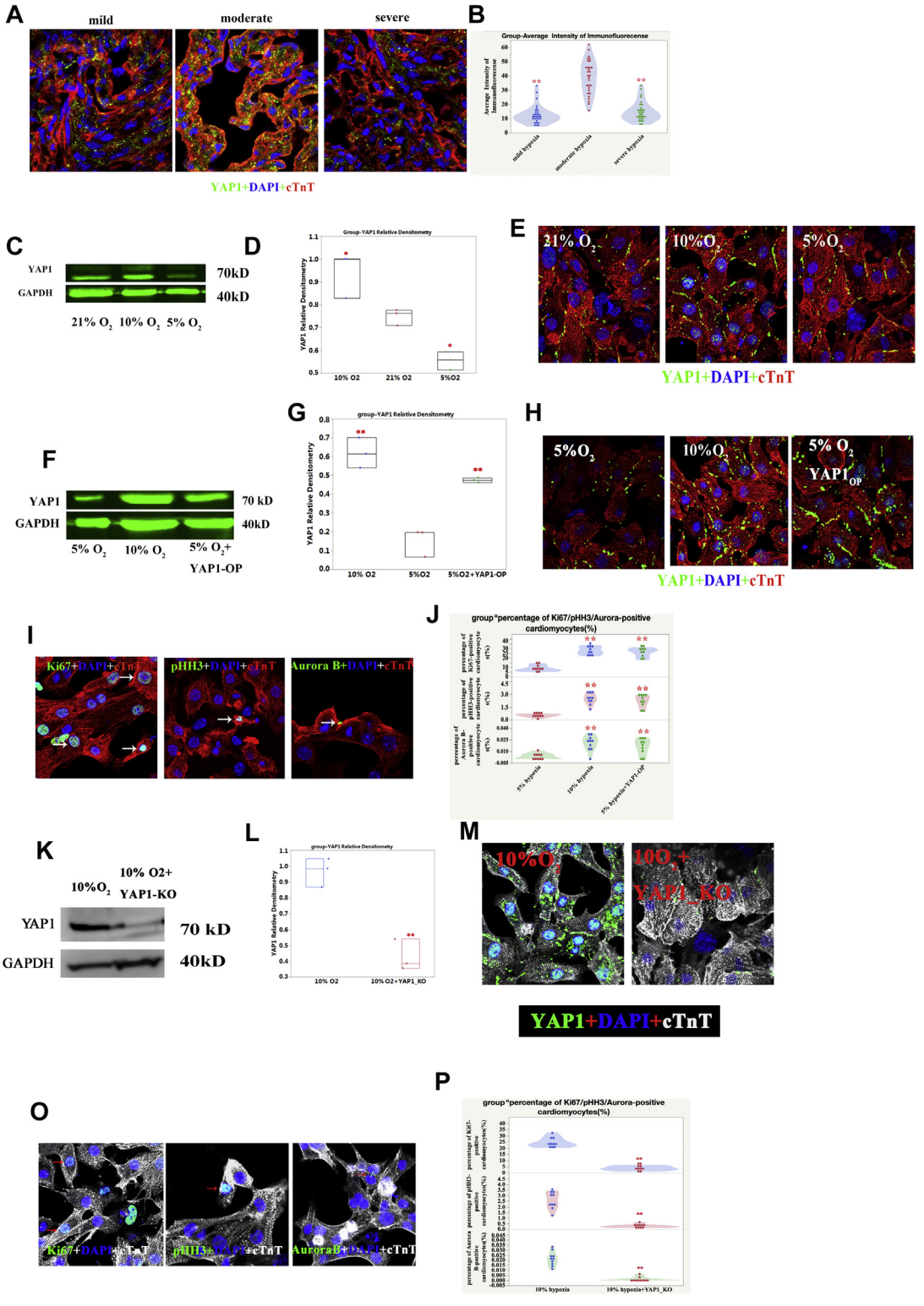

Continued on the next page

FIGURE 6 Reduced Oxidative DNA Damage After OP of YAP1 in 5% O_2-Treated Human iPSC-CMs

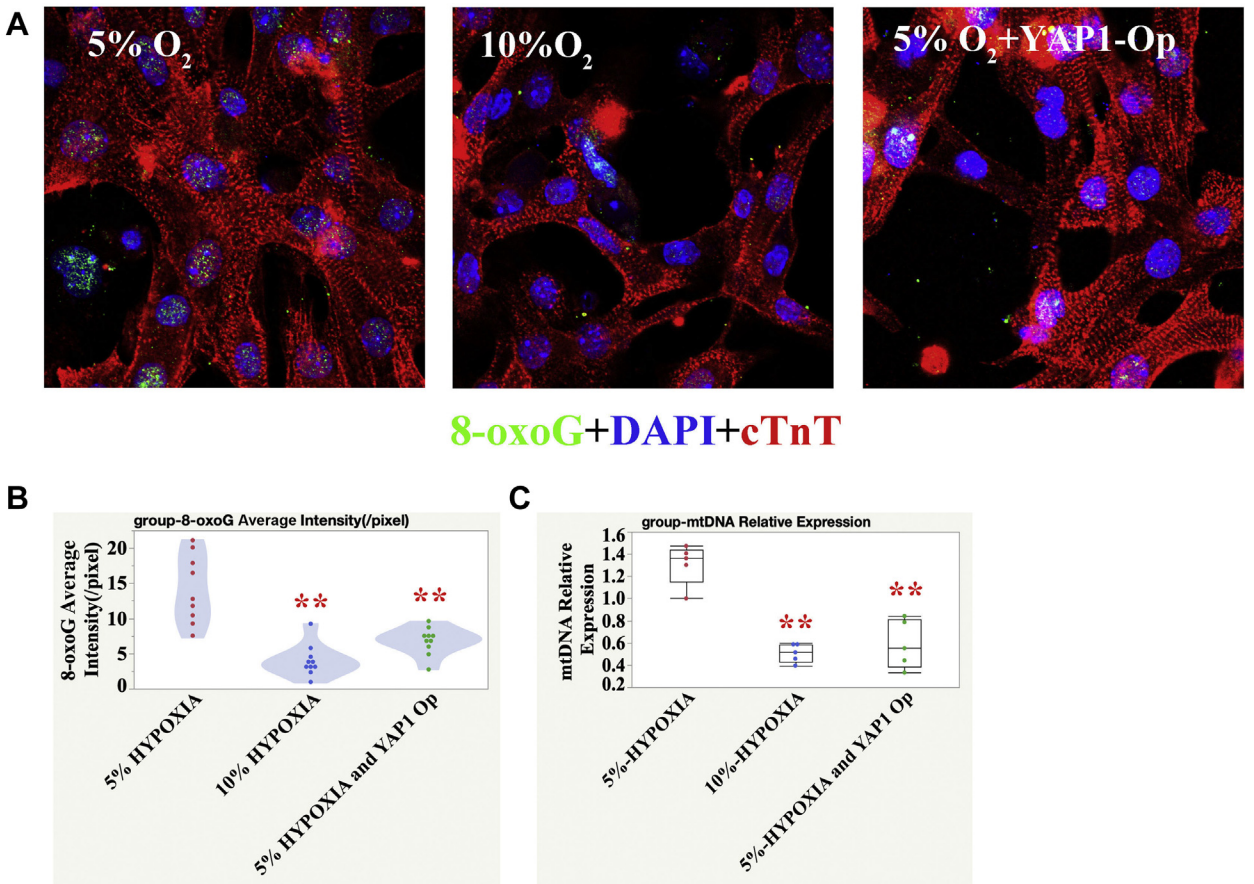

(A) Representative 8-oxoG IF in the 5% O_2, 10% O_2, 5% O_2-treated, and YAP1 OP group; cTnT **(red)**, 8-oxoG **(green)**, and DAPI **(blue)** stainings are shown. **(B)** Quantification of 8-oxoG IF intensity; 1-way ANOVA, SNK; **$p < 0.01$, $n = 10$ fields from 3 independent experiments compared with the 5% O_2 group. **(C)** Reduced mtDNA content in YAP1 OP group; 1-way ANOVA, SNK; **$p < 0.01$, $n = 5$ replicates compared with the 5% O_2 group. Abbreviations as in Figures 1 to 5.

DISCUSSION

CM proliferation contributes to post-natal heart growth in young humans, and their protective attributes are important in cardiac surgery and heart failure therapy (28). Currently, pharmacological treatment regimens are still the mainstay for heart failure in children. However, many of the drugs that

FIGURE 5 Continued

(A) Representative yes-associated protein 1 (YAP1) IF in human heart samples; cTnT **(red)**, YAP1 **(green)**, and DAPI **(blue)** stainings are shown. **(B)** Quantification of YAP1 IF intensity in human CMs; 1-way ANOVA, SNK; **$p < 0.01$, $n = 30$ slides, compared with the moderate group. **(C)** Higher expression of YAP1 in 10% O_2-treated group as measured by Western blot. **(D)** Quantification of YAP1 expression; *$p < 0.05$; $n = 3$ replicates. **(E)** Higher expression and nuclear location of YAP1 in 10% O2-treated group as measured by IF. **(F)** YAP1 overexpression (Op) in the 5% O_2-treated group as verified by the Western blot. **(G)** Quantification of YAP1 expression; **$p < 0.01$; $n = 3$ replicates. **(H)** YAP1 OP in the 5% O_2-treated group as verified by IF; cTnT **(red)**, YAP1 **(green)**, and DAPI **(blue)** stainings are shown. **(I)** Ki67-, pHH3-, and aurora B–positive human iPSC-CMs in 5% O_2-treated and YAP1 OP groups. **(J)** Quantification of Ki67-, pHH3-, and aurora B–positive CMs in the 10% O_2-treated, 5% O_2-treated, 5% O_2-treated and YAP1 OP group; 1-way ANOVA, SNK; **$p < 0.01$, $n = 10$ fields from 3 independent experiments compared with the 5% O_2 group. **(K)** YAP1 knockout (KO) in the 10% O_2-treated group as verified by Western blotting. **(L)** Quantification of YAP1 expression; **$p < 0.01$, $n = 3$ replicates. **(M)** YAP1 KO in the 10% O_2-treated group as verified by IF; cTnT **(white)**, YAP1 **(green)**, and DAPI **(blue)** staining are shown. **(N)** Representative Ki67-, pHH3-, and aurora B–positive human iPSC-CMs in 10% O_2-treated and YAP1 KO groups. **(O)** Quantification of Ki67-, pHH3-, and aurora B–positive CMs in the 10% O_2-treated, 10% O_2-treated, and YAP1 KO group; 1-way ANOVA, SNK; **$p < 0.01$, $n = 10$ fields from 3 independent experiments compared with the 10% O_2 group. Abbreviations as in Figures 1 to 4.

have been developed for heart failure (including beta-blockers and angiotensin-converting enzyme inhibitors) in adult patients are ineffective in pediatric patients (28,29). Furthermore, newer, more promising drugs have not been subjected to randomized clinical trials in pediatric patients (30,31). Because prevention is better than therapy, there is increasing awareness of the importance of protecting the young human heart. Therefore, new therapeutic paradigms for pediatric heart failure are now under investigation (32). This study is the first to focus on the relationship between CM proliferation and heart protection in children. We are hopeful that this research will provide a platform from which the potential pediatric heart failure therapies may be further investigated.

O_2 balance is extremely important in CHD therapy; too much or too little O_2 can be harmful to neonates with CHD. For example, excessive O_2 administration to newborns with single ventricle physiology can lead to circulatory collapse by increasing pulmonary blood flow at the expense of systemic perfusion, whereas insufficient O_2 may cause acidosis and subsequent brain damage (33). However, until now, researchers did not realize that balanced O_2 is also required for myocardial protection. During cardiopulmonary bypass, the myocardium is protected by 2 methods, hypothermia and potassium-induced electromechanical cardiac arrest, both of which reduce O_2 consumption in the heart (34,35). This study suggested that during the peri-operative period, moderate SaO_2 may be beneficial to CM cell cycle activities. Clinical investigations from other institutions also demonstrated that children who had severe SaO_2 deprivation needed more inotrope intervention (31). The underlying mechanism might be associated with oxidative DNA damage. We found that both too much and too little O_2 increased oxidative DNA damage (**Figures 3A to 3J**). As suggested by Schoots et al. (36), an imbalance between reactive O_2 species and antioxidants, because of hypoxia, caused damage to DNA.

In addition to observing how O_2 affects human CM proliferation, we investigated the effects of different concentrations of O_2 on the proliferation of iPSC-CMs in vitro. The results showed that 15% and 10% O_2 cultures significantly promoted the proliferation of CMs, but the effects of these 2 levels were similar. Conversely, 5% O_2 culture and a progressively hypoxic culture inhibited CM proliferation. These results suggested that a proper level of hypoxia was necessary during clinical monitoring, but excessive hypoxia or a rapid change in O_2 levels was not conducive to the recovery of the child's heart.

This study also helped reconcile the current international controversy of whether hypoxia is beneficial to CM proliferation. Our research showed that the answer is not simply yes or no but depends on the specific degree of hypoxia and whether it is acute or chronic progressive hypoxia. Studies at the Sadek Laboratory (University of Texas Southwestern Medical Center, Dallas, Texas) showed that progressive hypoxia in vivo is beneficial for CM proliferation. Our study contradicted those observations. There are 2 possible reasons for this. First, the differences between in vivo and in vitro experiments, and second, the Sadek Laboratory researchers induced progressive hypoxia by reducing the O_2 concentration by 1%/h, whereas we reduced it by 5% every other day. Thus, changes to the O_2 concentration in our study were more dramatic; such intense changes are not conducive to CM growth. Consistent with the previously mentioned observations, the manner of hypoxia exposure caused oxidative DNA damage (**Figures 3F to 3J**). Cai et al. (37) found that chronic intermittent hypoxia increased oxidative damage in the neonatal rat liver.

STUDY LIMITATIONS. Our results indicated that YAP1 served as an anti-oxidative DNA damage transcription factor in the regulation of CM proliferation. However, by what signaling pathway YAP1 plays such a role is still unknown, although some studies indicated that it might participate in the DNA base excision repair pathway (38). Another limitation of this study is that we still do not know how SaO_2 is converted into O_2 concentration in vitro. This limitation may impede the translation of our results into clinical application.

When considering the effects of hypoxia, the role of hypoxia-inducible factor 1 alpha must be considered. As expected, higher expression of hypoxia-inducible factor 1 alpha was found in the severe hypoxia group (Supplemental Figure S1); however, it has not been positively correlated with CM proliferation rate. The role of hypoxia-inducible factor-1 alpha in the regulation of CMs proliferation is complex. Paradis et al. (11) showed that when neonatal rat hearts were exposed to hypoxia in vivo, there was a significant increase in hypoxia-inducible factor-1 alpha protein but CMs proliferation was inhibited. Their results showed that in this process, endothelin-1 might be the major responsive factor. In contrast, Kimura et al. (39) showed that stabilization of hypoxia-inducible factor-1 alpha was

critical for stem or progenitor cells, mapping the proliferating CMs. How hypoxia-inducible factor-1 alpha, YAP1, and Pitx2 work together in the heart to regulate CMs proliferation needs more investigation.

CONCLUSIONS

Moderate hypoxia (SaO_2: 75% to 85%) is beneficial for the cell cycle activities of postnatal human CMs and a reduction in DNA damage and upregulation of YAP1 appear to be the underlying mechanisms.

ADDRESS FOR CORRESPONDENCE: Dr. Haifa Hong, Department of Thoracic and Cardiovascular Surgery, Shanghai Children's Medical Center, Shanghai Jiaotong University School of Medicine, 1678 Dongfang Road, Shanghai 200127, China. E-mail: hhfsmallboat@163.com. OR Dr. Jinfen Liu, Shanghai Institute for Pediatric Congenital Heart Diseases, Shanghai Children's Medical Center, Shanghai Jiaotong University School of Medicine, 1678 Dongfang Road, Shanghai 200127, China. E-mail: liujinfen2002@126.com.

PERSPECTIVES

COMPETENCY IN MEDICAL KNOWLEDGE: SaO_2 is one of the most important indexes of heart and brain protection during the peri-operative period. However, O_2 is deemed a double-edged sword regarding cardiac function and repair, and effects of hypoxia on CM proliferation are associated with its stage of development. The findings of this study demonstrated that moderate hypoxia benefits human CM proliferation both in vivo and in vitro. This phenomenon was associated with reduced oxidative DNA damage and upregulation of YAP1, the overexpression of which protects CM from oxidative DNA damage.

TRANSLATIONAL OUTLOOK: Moderate hypoxia benefits human CM proliferation, providing a rationale for why moderate hypoxia is targeted by many children's medical centers when children with CHD are being transported in preparation for cardiac surgery. A slower process to recover 100% SaO_2 may be considered for reperfusion after CPB. YAP1-modified RNA may be applied to protect the heart from oxidative DNA damage. Further research is necessary to develop more effective methods to promote CM proliferation because the CM turnover rate is low.

REFERENCES

1. Tennant PW, Pearce MS, Bythell M, Rankin J. 20-year survival of children born with congenital anomalies: a population-based study. Lancet 2010;375:649–56.

2. Hoffman JI, Kaplan S. The incidence of congenital heart disease. J Am Coll Cardiol 2002;39:1890–900.

3. Bolger AP, Coats AJ, Gatzoulis MA. Congenital heart disease: the original heart failure syndrome. Eur Heart J 2003;24:970–6.

4. Cerillo AG, Storti S, Kallushi E, et al. The low triiodothyronine syndrome: a strong predictor of low cardiac output and death in patients undergoing coronary artery bypass grafting. Ann Thorac Surg 2014;97:2089–95.

5. Ye L, Qiu L, Zhang H, Chen H, Jiang C, Hong H, Liu J. Cardiomyocytes in young infants with congenital heart disease: a three-month window of proliferation. Sci Rep 2016;15. 6:23188.

6. Ye L, Yin M, Xia Y, Jiang C, Hong H, Liu J. Decreased Yes-associated protein-1 (YAP1) expression in pediatric hearts with ventricular septal defects. PLoS One 2015;10:e0139712.

7. Mollova M, Bersell K, Walsh S, et al. Cardiomyocyte proliferation contributes to heart growth in young humans. Proc Natl Acad Sci U S A 2013;110:1446–51.

8. Watanabe T, Orita H, Kobayashi M, Washio M. Brain tissue pH, oxygen tension, and carbon dioxide tension in profoundly hypothermic cardiopulmonary bypass. Comparative study of circulatory arrest, nonpulsatile low-flow perfusion, and pulsatile low-flow perfusion. J Thorac Cardiovasc Surg 1989;97:396–401.

9. Ang YS, Srivastava D. Oxygen: double-edged sword in cardiac function and repair. Circ Res 2014;115:824–5.

10. Sun Y, Jiang C, Hong H, Liu J, Qiu L, Huang Y, Ye L. Effects of hypoxia on cardiomyocyte proliferation and association with stage of development. Biomed Pharmacother 2019;118:109391.

11. Paradis AN, Gay MS, Wilson CG, Zhang L. Newborn hypoxia/anoxia inhibits cardiomyocyte proliferation and decreases cardiomyocyte endowment in the developing heart: role of endothelin-1. PLoS One 2015;10:e0116600.

12. Puente BN, Kimura W, Muralidhar SA, et al. The oxygen-rich postnatal environment induces cardiomyocyte cell-cycle arrest through DNA damage response. Cell 2014;157:565–79.

13. Shivananda S, Kirsh J, Whyte HE, Muthalally K, McNamara PJ. Impact of oxygen saturation targets and oxygen therapy during the transport of neonates with clinically suspected congenital heart disease. Neonatology 2010;97:154–62.

14. Miquel J, Economos AC, Fleming J, Johnson JE Jr. Mitochondrial role in cell aging. Exp Gerontol 1980;15:575–91.

15. Turrens JF. Mitochondrial formation of reactive oxygen species. J Physiol 2003;552:335–44.

16. Srujana K, Begum SS, Rao KN, Devi GS, Jyothy A, Prasad MH. Application of the comet assay for assessment of oxidative DNA damage in circulating lymphocytes of tetralogy of Fallot patients. Mutat Res 2010;688:62–5.

17. Vidya G, Suma HY, Bhat BV, Chand P, Rao KR. Hypoxia induced DNA damage in children with isolated septal defect and septal defect with great vessel anomaly of heart. J Clin Diagn Res 2014;8:SC01–3.

18. Canseco DC, Kimura W, Garg S, et al. Human ventricular unloading induces cardiomyocyte proliferation. J Am Coll Cardiol 2015;65:892–900.

19. Del Re DP, Yang Y, Nakano N, et al. Yes-associated protein isoform 1 (Yap1) promotes cardiomyocyte survival and growth to protect against myocardial ischemic injury. J Biol Chem 2013;288:3977–88.

20. von Gise A, Lin Z, Schlegelmilch K, et al. YAP1, the nuclear target of Hippo signaling, stimulates heart growth through cardiomyocyte proliferation but not hypertrophy. Proc Natl Acad Sci U S A 2012;109:2394–9.

21. Xin M, Kim Y, Sutherland LB, et al. Hippo pathway effector Yap promotes cardiac regeneration. Proc Natl Acad Sci U S A 2013;110:13839–44.

22. Lehtinen MK, Yuan Z, Boag PR, et al. A conserved MST-FOXO signaling pathway mediates oxidative-stress responses and extends life span. Cell 2006;125:987–1001.

23. Xiao L, Chen D, Hu P, et al. The c-Abl-MST1 signaling pathway mediates oxidative stress-induced neuronal cell death. J Neurosci 2011;31:9611–9.

24. Phillips NR, Sprouse ML, Roby RK. Simultaneous quantification of mitochondrial DNA copy number and deletion ratio: a multiplex real-time PCR assay. Sci Rep 2014;4:3887.

25. Hesse M, Doengi M, Becker A, et al. Midbody positioning and distance between daughter nuclei enable unequivocal identification of cardiomyocyte cell division in mice. Circ Res 2018;123:1039–52.

26. Kanvah S, Joseph J, Schuster GB, Barnett RN, Cleveland CL, Landman U. Oxidation of DNA: damage to nucleobases. Acc Chem Res 2010;43:280–7.

27. Tao G, Kahr PC, Morikawa Y, et al. Pitx2 promotes heart repair by activating the antioxidant response after cardiac injury. Nature 2016;534:119–23.

28. Polizzotti BD, Ganapathy B, Walsh S, et al. Neuregulin stimulation of cardiomyocyte regeneration in mice and human myocardium reveals a therapeutic window. Sci Transl Med 2015;7:281ra45.

29. Burns KM, Byrne BJ, Gelb BD, et al. New mechanistic and therapeutic targets for pediatric heart failure: report from a National Heart, Lung, and Blood Institute Working Group. Circulation 2014;130:79–86.

30. Shaddy RE, Boucek MM, Hsu DT, et al. Pediatric Carvedilol Study Group. Carvedilol for children and adolescents with heart failure: a randomized controlled trial. JAMA 2007;298:1171–9.

31. Rossano JW, Cabrera AG, Jefferies JL, Naim MP, Humlicek T. Pediatric Cardiac Intensive Care Society 2014 consensus statement: pharmacotherapies in cardiac critical care chronic heart failure. Pediatr Crit Care Med 2016;17 3 Suppl 1:S20–34.

32. Richmond ME, Easterwood R, Singh RK, et al. Low-dose donor dopamine is associated with a decreased risk of right heart failure in pediatric heart transplant recipients. Transplantation 2016;100:2729–34.

33. Brooks PA, Penny DJ. Management of the sick neonate with suspected heart disease. Early Hum Dev 2008;84:155–9.

34. Baikoussis NG, Papakonstantinou NA, Verra C, et al. Mechanisms of oxidative stress and myocardial protection during open-heart surgery. Ann Card Anaesth 2015;18:555–64.

35. Bigelow WG, Lindsay WK, Greenwood WF. Hypothermia; its possible role in cardiac surgery: an investigation of factors governing survival in dogs at low body temperatures. Ann Surg 1950;132:849–66.

36. Schoots MH, Gordijn SJ, Scherjon SA, van Goor H, Hillebrands JL. Oxidative stress in placental pathology. Placenta 2018;69:153–61.

37. Cai C, Aranda JV, Valencia GB, Xu J, Beharry KD. Chronic intermittent hypoxia causes lipid peroxidation and altered phase 1 drug metabolizing enzymes in the neonatal rat liver. React Oxyg Species (Apex) 2017;3:218–36.

38. Rowe LA, Degtyareva N, Doetsch PW. Yap1: a DNA damage responder in Saccharomyces cerevisiae. Mech Ageing Dev 2012;133:147–56.

39. Kimura W, Xiao F, Canseco DC, et al. Hypoxia fate mapping identifies cycling cardiomyocytes in the adult heart. Nature 2015;523:226–30.

KEY WORDS blood oxygen saturation, cardiomyocyte, congenital heart disease, pediatric patients, proliferation

APPENDIX For supplemental figures and tables, please see the online version of this paper.